Biochimica et Biophysica Acta 1852 (2015) 1410–1419

Contents lists available at ScienceDirect

Biochimica et Biophysica Acta

journal homepage: www.elsevier.com/locate/bbadis

Altered ROS production, NF-κB activation and interleukin-6 gene expression induced by electrical stimulation in dystrophic *mdx* skeletal muscle cells

Carlos Henríquez-Olguín [a,c,1], Francisco Altamirano [a,b,*,1], Denisse Valladares [a], José R. López [b], Paul D. Allen [b], Enrique Jaimovich [a,**]

[a] Centro de Estudios Moleculares de la Célula, ICBM, Facultad de Medicina, Universidad de Chile, Santiago 8389100, Chile
[b] Department of Molecular Biosciences, School of Veterinary Medicine, University of California at Davis, Davis, CA, USA
[c] Laboratorio Ciencias del Ejercicio, Clínica MEDS, Santiago, Chile

ARTICLE INFO

Article history:
Received 3 December 2014
Received in revised form 6 March 2015
Accepted 30 March 2015
Available online 7 April 2015

Keywords:
Duchenne muscular dystrophy
NF-κB
Reactive oxygen species
Interleukin-6
Membrane depolarization
Calcium

ABSTRACT

Duchenne muscular dystrophy is a fatal X-linked genetic disease, caused by mutations in the dystrophin gene, which cause functional loss of this protein. This pathology is associated with an increased production of reactive oxygen (ROS) and nitrogen species. The aim of this work was to study the alterations in NF-κB activation and interleukin-6 (IL-6) expression induced by membrane depolarization in dystrophic *mdx* myotubes. Membrane depolarization elicited by electrical stimulation increased p65 phosphorylation, NF-κB transcriptional activity and NF-κB-dependent IL-6 expression in *wt* myotubes, whereas in *mdx* myotubes it had the opposite effect. We have previously shown that depolarization-induced intracellular Ca^{2+} increases and ROS production are necessary for NF-κB activation and stimulation of gene expression in *wt* myotubes. Dystrophic myotubes showed a reduced amplitude and area under the curve of the Ca^{2+} transient elicited by electrical stimulation. On the other hand, electrical stimuli induced higher ROS production in *mdx* than *wt* myotubes, which were blocked by NOX2 inhibitors. Moreover, mRNA expression and protein levels of the NADPH oxidase subunits: $p47^{phox}$ and $gp91^{phox}$ were increased in *mdx* myotubes. Looking at ROS-dependence of NF-κB activation we found that in *wt* myotubes external administration of 50 μM H_2O_2 increased NF-κB activity; after administration of 100 and 200 μM H_2O_2 there was no effect. In *mdx* myotubes there was a dose-dependent reduction in NF-κB activity in response to external administration of H_2O_2, with a significant effect of 100 μM and 200 μM, suggesting that ROS levels are critical for NF-κB activity. Prior blockage with NOX2 inhibitors blunted the effects of electrical stimuli in both NF-κB activation and IL-6 expression. Finally, to ascertain whether stimulation of NF-κB and IL-6 gene expression by the inflammatory pathway is also impaired in *mdx* myotubes, we studied the effect of lipopolysaccharide on both NF-κB activation and IL-6 expression. Exposure to lipopolysaccharide induced a dramatic increase in both NF-κB activation and IL-6 expression in both *wt* and *mdx* myotubes, suggesting that the altered IL-6 gene expression after electrical stimulation in *mdx* muscle cells is due to dysregulation of Ca^{2+} release and ROS production, both of which impinge on NF-κB signaling. IL-6 is a key metabolic modulator that is released by the skeletal muscle to coordinate a multi-systemic response (liver, muscle, and adipocytes) during physical exercise; the alteration of this response in dystrophic muscles may contribute to an abnormal response to contraction and exercise.

1. Introduction

Duchenne muscular dystrophy (DMD) is a lethal X-linked human genetic muscular disorder caused by mutations in the dystrophin gene that lead to the absence of dystrophin protein [1]. DMD is a severe and progressive muscle wasting disease leading to wheelchair dependence and premature death [2]. DMD patients have an abnormal response to exercise compared to control subjects [3,4] and it has been shown that running exercise induces rapid muscle damage [5], cell death and worsening of the muscle pathology [4]. However, beneficial effects of exercise through utrophin upregulation in dystrophic patients have been reported as well [6].

A hallmark feature of DMD pathology is the excessive inflammation observed in the skeletal muscles due to immune cell infiltrates and an increase in inflammatory mediators [7,8]. Interleukin-6 (IL-6) is a ubiquitously expressed cytokine with either pro- or anti-inflammatory

* Correspondence to: F. Altamirano, Department of Molecular Biosciences, School of Veterinary Medicine, University of California Davis, 1089 Veterinary Medicine Drive, VM3B, Davis, CA 95616, USA.
** Correspondence to: E. Jaimovich, Instituto de Ciencias Biomédicas, Facultad de Medicina, Universidad de Chile, Casilla 70005, Santiago 7, Chile.
E-mail addresses: fcoaltamirano@ucdavis.edu, fcoaltamirano@gmail.com (F. Altamirano), ejaimovi@med.uchile.cl (E. Jaimovich).
[1] Both authors contributed equally to this work.

http://dx.doi.org/10.1016/j.bbadis.2015.03.012
0925-4439/

effects depending on the tissue microenvironment and the concentration [9]. In DMD patients, as well as in the *mdx* mouse (a DMD model) elevated IL-6 levels have been found both in plasma and muscle [10,11]. Recently, we reported that there were no differences in IL-6 gene expression between *wt* and *mdx* myotubes [12], suggesting that it is the immune cell infiltrates rather than the skeletal muscles themselves that produce the elevated levels of this cytokine.

In normal patients and animals, IL-6 plasma levels are increased by exercise and it appears that contracting muscles are the source of this increase [13]. IL-6 plays a central role in muscle communication with several tissues such as the liver, adipose cells, and other muscles to increase energy supply during exercise, making it an essential metabolic regulator [13,14]. Several intracellular signaling pathways have been related to IL-6 expression in the skeletal muscle including NF-κB activation, and reactive oxygen species (ROS) production [14,15]. In skeletal muscle cells, membrane depolarization activates NF-κB by a mechanism involving Ca^{2+} release from the sarcoplasmic reticulum (SR) and ROS production [16]. ROS and reactive nitrogen species (RNS) have long been implicated in cellular damage and we have previously reported an increase in iNOS expression and nitric oxide (NO) production in *mdx* myotubes [12]. ROS and RNS have also emerged as important physiological signaling molecules that modify receptor stimulation, enzymatic activity and gene expression in skeletal muscle cells [17]. In normal skeletal muscle NADPH oxidase (NOX) is a major source of ROS both at rest and during contraction [18–20]. NOX2 is found mainly in transverse tubules [21] and consists in regulatory cytosolic units ($p47^{phox}$, $p67^{phox}$, and $p40^{phox}$), a GTPase protein (rac 1), and the catalytic membrane-bound subunits: $gp91^{phox}$ and $p22^{phox}$. Several studies have shown that NOX2 activity is altered in *mdx* muscle and could play an important role in dystrophic pathophysiology [22,23].

Until now, there have been no studies addressing the molecular mechanism involved in NF-κB activation and IL-6 production elicited by membrane depolarization in dystrophic skeletal muscle cells. The aim of this work was to study the alterations in both NF-κB activation and IL-6 gene expression induced by ES between *wt* and *mdx* myotubes.

2. Material and methods

2.1. Cell culture

Primary myotubes from *wild type* (*C57BL/6*) and *mdx* (C57BL/10ScSn-Dmd<*mdx*>/J) mice were isolated according to the method of Rando and Blau [24]. The myoblasts were grown and differentiated as described previously [25]. For experiments myoblasts were seeded in matrigel-coated dishes or coverslips. When cells reached approximately 70% confluence, growth medium was replaced with differentiation medium (DMEM low glucose, 4% heat inactivated horse serum and 1× Pen–Strep–Glutamine solution) to induce myoblast differentiation. The medium was changed every two days and cells were used for experimental determinations at days 3–4 of differentiation.

2.2. Swimming exercise protocol

A 1-liter beaker filled with water at room temperature was used as swimming pool. Briefly, *wt* and *mdx* mice were gently placed in the water to perform 1 h of swimming (without any weight on the tail). Later, mice were removed immediately from the swimming pool, dried gently with paper towels and returned to their cages. After 2 h the animals were euthanized, their diaphragm muscles were dissected and RNA was extracted using the TRIzol reagent according to the manufacturer's instructions.

2.3. Electric stimulation protocol

Myotubes were stimulated with a stimulation device, that consists of six rows of platinum wires, intercalated 0.5 cm apart, with alternate polarity across a circular Teflon holder that fits in the dish. This was connected to a Grass S48 pulse generator, as described previously [26]. The protocol for electrical stimulation (ES) used was a single train of 250 square wave pulses of 0.5 ms duration at a frequency of 20 Hz (12.5 s total). This protocol was previously shown to be effective in inducing both Ca^{2+} signaling and gene expression in skeletal muscle cells [26]. For some experiments, high potassium solution (85 NaCl, 60 KCl, 2.5 $CaCl_2$, 1 $MgCl_2$, 5.6 glucose, 10 HEPES–Tris, pH 7.4) was used to study the magnitude of NF-κB activation. Depolarization proceeded during 1 min in the high potassium solution, returning to normal physiological solution (140 NaCl, 5 KCl, 2.5 $CaCl_2$, 1 $MgCl_2$, 5.6 glucose, 10 HEPES–Tris, pH 7.4). Protein samples were obtained 30 or 60 min after high potassium depolarization protocol.

2.4. Western blot

Total protein lysates were prepared from differentiated myotubes by homogenizing them in a lysis buffer containing 20 mM Tris–HCl (pH 7,5), 1% Triton X-100, 1 mM EDTA, 1 mM EGTA, 20 mM NaF, 1 mM $Na_2P_2O_7$, 10% glycerol, 150 mM NaCl, 10 mM Na_3VO_4, 1 mM PMSF and protease inhibitors (Complete™, Roche Applied Science). Proteins were separated using SDS-PAGE and transferred to PVDF membranes. The following primary antibodies and their dilutions were used: $gp91^{phox}$ (1:1000; Santa Cruz Biotechnology); p-p65 (Ser536; 1:2000; Cell Signaling), p65 (total; 1:2000; Cell Signaling), IκBα (1:1000; Cell Signaling), β-tubulin (1:1000, Sigma Aldrich) and GAPDH (1:10,000; Cell Signaling). The protein bands in the blots were visualized using either HRP secondary antibodies and autoradiography films or quantified with Odyssey Imaging System (Li-COR Biosciences).

2.5. NF-κB luciferase reporter activity determinations

Both *wt* and *mdx* myoblasts were transduced with a lentivirus containing 5 tandem NF-κB binding site repeats cloned upstream of a luciferase reporter gene and populations that stably expressed the transgene were selected using G418, as described previously [12]. Myotubes were stimulated in differentiation media. Luciferase activity was determined using the luciferase reporter assay system (Promega) according to the manufacturer's instructions. Light detection was carried out in a Berthold F12 luminometer. Results were normalized with total protein and the ratio "luciferase mg^{-1}" was shown.

2.6. ELISA

Culture media (DMEM with 5% heat inactivated horse serum and antibiotics) were changed one day before the experiment to allow basal IL-6 release stabilization. The ES protocol was applied as described above and after 2 h media samples (1 mL) were collected from both an ES-stimulated dish and a control dish (no media change before the experiment). Supernatants were spun at 10,000 ×*g* for 1 min to remove any cellular debris and kept on ice. ELISA was carried out immediately using a Mouse IL-6 High Sensitivity ELISA Kit (Affymetrix eBioscience #BMS603HS) according to the manufacturer's instructions. Total proteins were extracted with lysis buffer and the protein concentration was assessed with the BCA method. IL-6 levels (pg/mL) were normalized to the total protein (mg).

2.7. Ca^{2+} transients

Differentiated myotubes were loaded with 5 μM with Fluo3-AM at 37 °C, 30 min in normal physiological solution. Image series during stimulation experiments were obtained with an inverted microscope

(Olympus T041) with epifluorescence illumination (XCite® Series 120) equipped with a CCD cooled camera (QImaging, Retiga 2000R) every 0.7 s at room temperature (RT). A filter Wheel (Lambda 10-2, Sutter Instruments) was used to filter 484-nm wavelength. The experiments were performed in Krebs–Ringer's solution (in mM: 140 NaCl, 5 KCl, 1 $MgCl_2$, 1 $CaCl_2$, 5.5 glucose, 10 HEPES, pH 7.4). Fluorescence images were analyzed with ImageJ software (NIH, Bethesda) and the average cell fluorescence, F, was calculated from selected regions of interest (ROI). Fluorescence data (F) normalized with respect to basal fluorescence (F_0) were expressed as $[F - F_0] / F_0$ ($\Delta F/F_0$).

2.8. ROS production

Myotubes were loaded with 5 μM CM-H_2DCFA for 15 min at 37 °C in imaging solution. The cells on coverslips were washed with Ringer solution and placed on the stage of confocal microscope (Carl Zeiss Pascal 5, LSM) at RT. The experiments were performed in Krebs–Ringer's solution (in mM: 140 NaCl, 5 KCl, 1 $MgCl_2$, 1 $CaCl_2$, 5.5 glucose, 10 HEPES, pH 7.4). CM-H_2DCFA fluorescence was detected using excitation at 488 nm and emission at 510–540 nm. In all measurements, a control with laser excitation only was performed. The laser illumination was kept at a minimum to prevent light activation of the dye. Fluorescence images were analyzed with ImageJ software (NIH, Bethesda) and the average cell fluorescence, F, was calculated from selected regions of interest (ROI). Fluorescence data (F) normalized with respect to basal fluorescence (F_0) of *wt* myotubes were expressed as $[F - F_0] / F_0$ ($\Delta F/F_0$).

2.9. Real time PCR

Total RNA from myotube cultures was isolated with TRIzol reagent (Invitrogen) and cDNA was prepared using SuperScript II (Invitrogen) according to the manufacturer's protocol. Real-time PCR was performed using a Stratagene Mx3000P as follows: Primers were used at 400 nM final concentrations and 2 μL of cDNA reaction together with the appropriate primers was added to 10 μL Brilliant III UltraFast SYBR green QPCR Master mix (Agilent Technologies) to a total volume of 20 μL. No-template control (NTC) reactions were also prepared for each gene. The cycling parameters for all genes were the following: 95 °C for 3 min, then 50 cycles of 95 °C for 20 s, and 60 °C for 20 s. Expression values were normalized to GAPDH and are reported in units of $2^{-\Delta\Delta Ct}$ [27]. PCR products was verified by melting-curve analysis and resolved by electrophoresis on 2% agarose gel and stained with ethidium bromide. The $p47^{phox}$, $gp91^{phox}$, IL-6 and GAPDH mRNA transcripts were quantified using oligonucleotide primers designed based on sequences published in NCBI GenBank with the open-source PerlPrimer software [28], using the following primers:

$gp91^{phox}$ 5′-TCACATCCTCTACCAAAACC-3′ and 5′-CCTTTATTTTTCCCCATTCT-3′;

$p47^{phox}$ 5′-AGAACAGAGTCATCCCACAC-3′ and 5′-GCTACGTTATTCTTGCCATC-3′;

gapdh 5′-CTCATGACCACAGTCCATGC-3′ and 5′-TTCAGCTCTGGGATGACCTT-3′;

IL-6 5′-CCAATTTCCAATGCTCTCCT 3′ and 5′-ACCACAGTGAGGAATGTCCA-3′.

2.10. Statistics

All values are expressed as mean ± SEM from at least 3 different independent determinations. Data were normalized to *wt* values at control conditions. Statistical analysis was performed using either unpaired two-tailed *t* test or ANOVA-with Dunnett's correction to determine significance ($P < 0.05$).

3. Results

3.1. Depolarization-induced NF-κB activation is impaired in mdx myotubes

Membrane depolarization by either ES or high extracellular potassium has been shown to activate NF-κB in *wt* skeletal muscle cells [16]. In order to study any alterations in NF-κB activation we studied the levels of p-p65 (Ser536), p65 and IκBα by western blot as well as NF-κB transcriptional activity. In *wt* myotubes electrical stimulation (250 pulses of 0.5 ms of duration at 20 Hz frequency) increased p-p65 levels at 30 min ($P < 0.05$), which returned to nonsignificant levels above baseline at 60 min (Fig. 1A and B) but no significant changes in total p65 and IκBα levels were observed at any time point (Fig. 1C and D). Similar results were observed in *wt* myotubes after potassium depolarization protocol at 30 min, however the increase in p-p65 levels did not reach statistical significance, probably due to the differences in the duration of the depolarization protocol and its effects in the time course of NF-κB activation (Fig. 1). In *mdx* myotubes, electrical stimuli did not modify p-p65, p65 or IκBα levels (Fig. 1A–D). NF-κB transcriptional activity, assessed by a luciferase reporter, increased by 2-fold at 12 h post-ES in *wt* myotubes ($P < 0.05$) (Fig. 1E), and had the opposite effects on NF-κB transcriptional activity, reducing it by 2-fold after stimulation at 12 h ($P < 0.05$) in dystrophic myotubes (Fig. 1E). NF-κB transcriptional activity was elevated in *mdx* myotubes at resting conditions, and this was correlated with reduced IκBα levels, reduced p-p65 (Fig. 1B, D and E).

3.2. Depolarization-induced IL-6 expression is altered in mdx myotubes

Membrane depolarization increases IL-6 gene expression in human and rat myotubes [14,29] and this increased expression requires activation of NF-κB [14]. Here we studied the changes in IL-6 mRNA levels induced by ES by real time PCR. In *wt* myotubes ES significantly increased IL-6 mRNA levels by 2.9 and 2.5-fold at 2 and 3 h post-stimuli, respectively ($P < 0.001$ and $P < 0.01$ compared to basal value) (Fig. 2A). On the contrary, ES reduced IL-6 mRNA levels in *mdx* myotubes, reaching a 78% reduction at 3 h post-stimuli ($P < 0.01$) (Fig. 2A).

3.3. NF-κB is involved in depolarization-induced IL-6 expression

Some studies have shown that IL-6 gene expression can be controlled by NFAT and AP-1 rather than NF-κB [13]. To determine the effects of NF-κB inhibition on IL-6 gene expression, we applied 50 μM SN50, a cell permeable NF-κB inhibitory peptide [30], 30 min before ES and kept it on the cells during the entire experiment. IL-6 was significantly increased 2 h after ES in *wt* myotubes, compared to un-stimulated myotubes ($P < 0.05$) (Fig. 2B) and SN50 treatment prevented the increase in IL-6 mRNA. In addition, SN50 treatment prevented the reduction in IL-6 mRNA levels after membrane depolarization in *mdx* myotubes (Fig. 2B). Secreted IL-6 levels were measured in culture supernatants from *wt* and *mdx* myotubes using a high sensitivity ELISA kit. ES significantly increased the IL-6 secretion from 8.5 ± 1.4 to 14.1 ± 1.1 pg/mg protein ($P < 0.05$) in *wt* myotubes (Fig. 2C). Surprisingly, we found that the basal IL-6 release was augmented in *mdx* myotubes to 95.9 ± 4.8 pg/mL despite the fact that basal IL-6 mRNA was not different from *wt* myotubes. However, after ES there was no significant change in *mdx* myotubes ($P > 0.05$), supporting our hypothesis that dystrophic skeletal muscle cells fail to increase the expression and release of IL-6 after membrane depolarization. This suggests that there is an altered secretion route for IL-6 that is normally pre-pooled inside the cell and released during exercise [31].

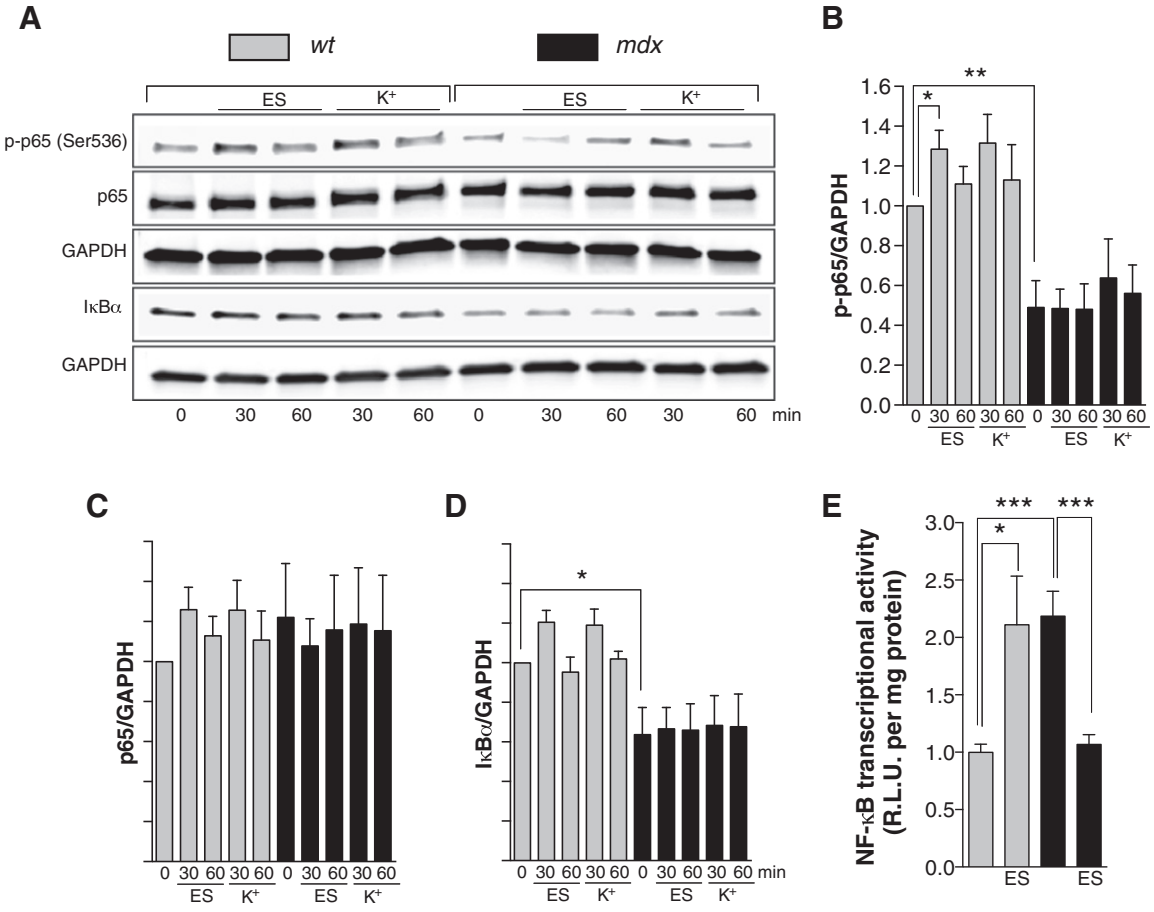

Fig. 1. NF-κB activation after membrane depolarization is impaired in *mdx* myotubes. Cells were stimulated at 250 pulses of 0.5 ms of duration at 20 Hz or with 60 mM K^+ solution for 1 min. Then, myotubes were returned to imaging solution and lysed at 30 and 60 min. A. Representative western blots. Quantification of p-p65/GAPDH (B), p65/GAPDH (C) and IκBα/GAPDH (D) ratios (n = 4). E. NF-κB transcriptional activity (luciferase assay) at 12 h (n = 7–9). * = $P < 0.05$, ** = $P < 0.01$ (indicated or versus basal *wt* value).

3.4. Dystrophic diaphragms fail to express IL-6 expression after swimming exercise in mice

To examine whether the alteration of IL-6 expression was relevant to exercised skeletal muscles of dystrophic mice we used a swimming protocol to assess these phenomena in vivo. Mice were allowed to swim for 1 h and then, 2 h post-exercise, they were euthanized, mRNA was extracted and the IL-6 expression was assessed by real time PCR. As we expected, swimming exercise increased IL-6 expression by 2.9-fold ($P < 0.05$) in diaphragm muscles from *wt* mice (Fig. 2D). Basal IL-6 expression was elevated in dystrophic diaphragms by 3.7-fold compared to *wt*, and swimming exercise did not modify its expression level ($P > 0.05$).

3.5. Ca^{2+} transients after membrane depolarization

We have previously demonstrated that depolarization-induced NF-κB activation depends on changes in both intracellular Ca^{2+} concentration and ROS production [16,32]. We studied the Ca^{2+} transient elicited by ES using Fluo3-AM and epifluorescence microscopy. Dystrophic *mdx* myotubes showed a reduced area under the curve of the Ca^{2+} transient elicited by ES (≈50%, $P < 0.001$ see Fig. 3).

3.6. ROS production induced by depolarization is higher in mdx myotubes

To study the ROS production induced by ES, myotubes were loaded with CM-H_2DCFDA (5 μM), a nonspecific *redox* probe that emits fluorescence when oxidized. The fluorescence changes over time were determined by confocal microscopy. Basal florescence was increased in *mdx* myotubes (Fig. S1). Membrane depolarization by ES increased ROS production in both *wt* and *mdx* myotubes (Fig. 4A and B) but the rate of ROS production was significantly higher in *mdx* myotubes compared with *wt* myotubes (0.49 vs 0.32 afu/s, $P < 0.05$) (Fig. 4C).

3.7. Catalytic and regulatory subunits of NADPH oxidase are over-expressed in mdx myotubes

NOX2 is the main ROS source in skeletal muscle cells [33], previous studies have shown an overexpression in *mdx* muscles [22,23]. In order to establish the contribution of NOX2 to depolarization-induced ROS production, we applied one of two NOX2 inhibitors (gp91-dstat peptide (1 μM) or apocynin (5 μM)) prior to and during ES. Both gp91-dstat and apocynin blunted the ROS production after ES ($P < 0.001$), but the inhibitory effect of NOX2 inhibitors was higher in *mdx* myotubes than in *wt*. We then measured the mRNA expression of two key subunits of the NADPH oxidase enzyme complex; regulatory subunit $p47^{phox}$ and catalytic subunit $gp91^{phox}$, and found that both the $p47^{phox}$ and $gp91^{phox}$ mRNA levels were increased by 9-fold ($P < 0.01$) and 2-fold ($P < 0.05$), respectively in *mdx* compared to *wt* myotubes under resting conditions (Fig. 4E). To confirm this we quantitated the $gp91^{phox}$ catalytic subunit protein levels by western blot. In *mdx* myotubes, $gp91^{phox}$ expression was 8.5-fold higher compared with *wt* myotubes ($P < 0.05$) (Fig. 4F and G).

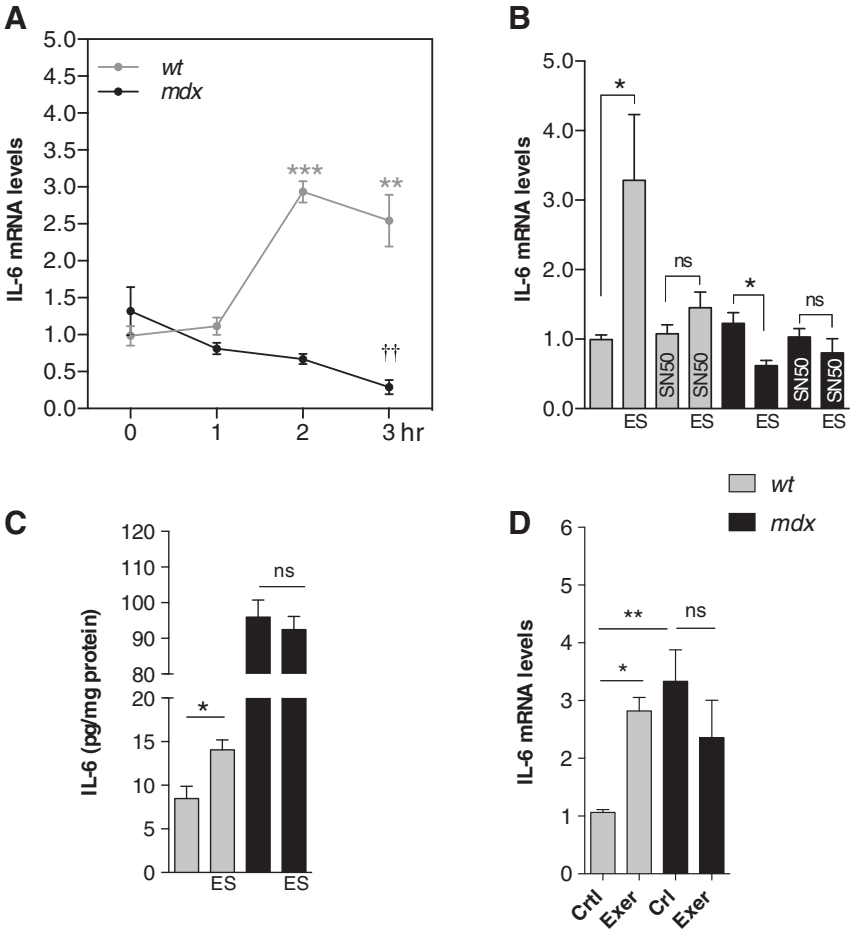

Fig. 2. IL-6 expression and secretion are defective in *mdx* myotubes. A. IL-6 expression determined by real time PCR at 1, 2 and 3 h post-stimuli (n = 3). B. Effect of SN50 (NF-κB inhibitor, 50 μM) on depolarization-induced IL-6 expression (n = 3–7). C. IL-6 secreted levels measured after ES in *wt* and *mdx* myotubes (n = 6). D. IL-6 expression in diaphragms from either swim-exercised or control mice (n = 6). * = $P < 0.05$, ** = $P < 0.01$, *** = $P < 0.001$ (indicated or versus basal *wt* value). †† = $P < 0.01$ (versus basal *mdx* value) and ns, no significant difference.

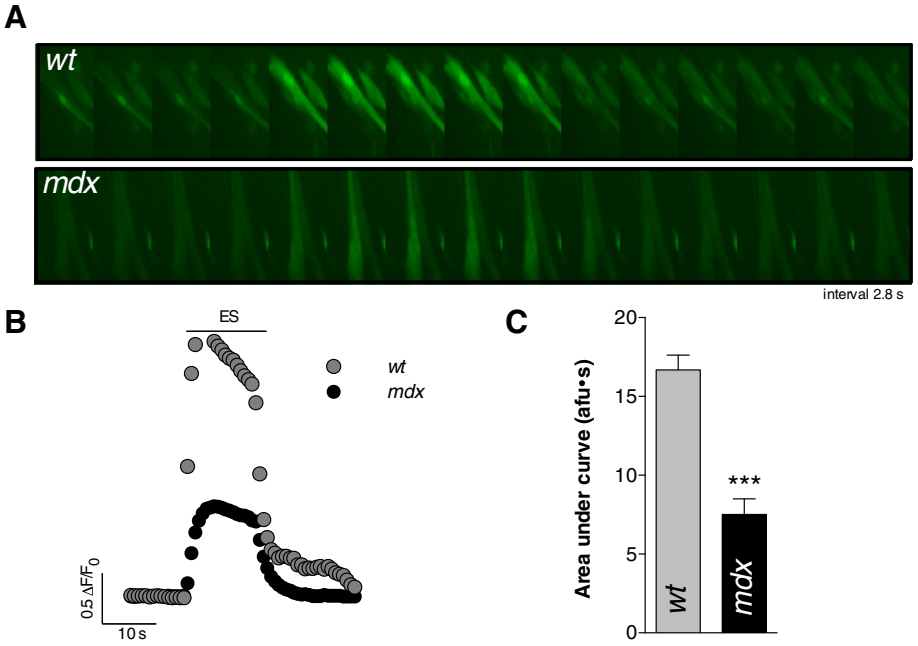

Fig. 3. Ca^{2+} transients elicited by ES in both *wt* and *mdx* myotubes. A. Representative fluorescence images and B. representative traces obtained with Fluo3-AM and epifluorescence microscopy. C. Quantification of the area under the curve of the evoked transients. (n = 40 cells for *wt* and n = 40 for *mdx* myotubes, from at least 3 independent cultures, respectively). *** = $P < 0.001$.

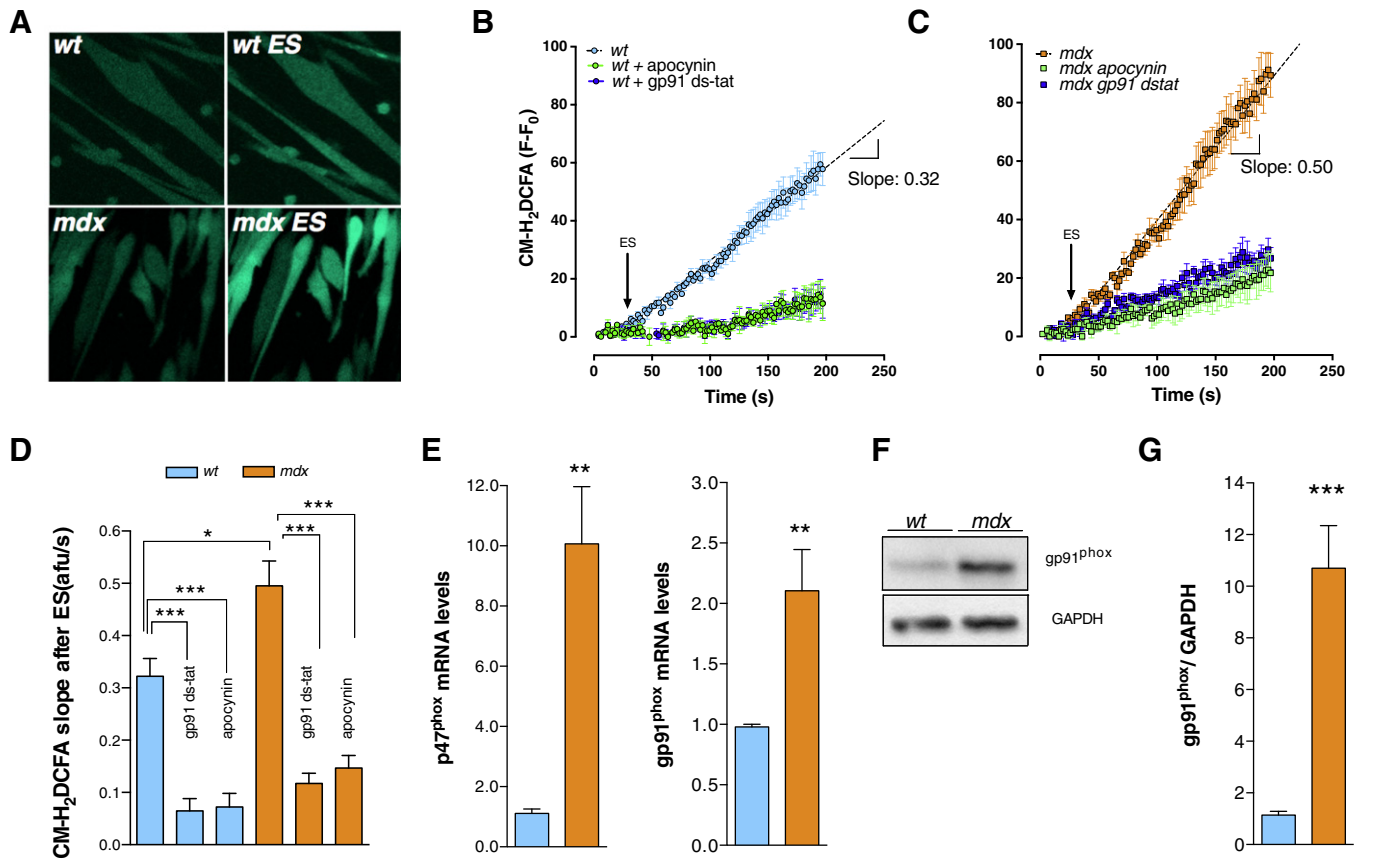

Fig. 4. Depolarization-induced ROS production is increased in *mdx* myotubes due to NOX2 overexpression. Cells were preloaded with CM-H_2DCFDA and stimulated at 250 pulses of 0.5 ms of duration at 20 Hz frequency in physiological solution at RT. Average traces obtained in both *wt* myotubes (A) and *mdx* myotubes (B) with either apocynin or gp91-dstat. Arrow approximately indicates the ES starting time. C. Slope quantification of CM-DCFDA fluorescent signal in both *wt* and *mdx* myotubes (n = 12 and n = 4 cells, for ROIs and cells respectively, 3 different preparations.). mRNA levels of $p47^{phox}$ (D) and $gp91^{phox}$ (E) subunits assessed by real time PCR (n = 3). F. Representative western blot showing $gp91^{phox}$ overexpression in *mdx* myotubes and G. quantification of $gp91^{phox}$ western blot (n = 5). * = $P < 0.05$, ** = $P < 0.01$, and *** = $P < 0.001$ (indicated or versus basal *wt* value).

3.8. ROS differentially modulate NF-κB activation in wt and mdx myotubes

ROS have been reported to both activate and to repress NF-κB signaling depending on the intracellular pathway activated and the cell type [34]. To determine whether ROS play a role in NF-κB activity in *wt* and *mdx* myotubes, we evaluated their response to exogenous H_2O_2. NF-κB luciferase activity was then assessed 12 h after ROS stimulation at different doses of H_2O_2. In *wt* myotubes 50 μM H_2O_2 significantly increased NF-κB activity ($P < 0.05$) but higher doses did not show any significant effect (Fig. 5A). In *mdx* myotubes, 50 μM H_2O_2 did not induce any changes in NF-κB activity, whereas at 100 and 200 μM H_2O_2 there was a significant reduction in NF-κB activity ($P < 0.05$, and $P < 0.01$, respectively) (Fig. 5A).

3.9. NOX2 inhibition reduces the effects of ES on NF-κB activity

To establish a correlation between the NOX2-dependent ROS production and NF-κB activation, cells were treated with apocynin (5 μM) for 30 min before and during ES. Apocynin treatment reduced basal NF-κB activity by ~51% in *mdx* myotubes, without any significant effect in *wt* myotubes (Fig. 5B). In addition, apocynin blunted the NF-κB activation after membrane depolarization in *wt* myotubes ($P < 0.001$), while in *mdx* myotubes, apocynin treatment reduced the inhibitory effects of ES on NF-κB activity ($P < 0.05$) (Fig. 5B).

3.10. NOX2 inhibition reduces depolarization effects on IL-6 gene expression

To establish a correlation between NOX2-dependent ROS production and IL-6 gene expression, we treated myotubes either with gp91-dstat (1 μM) or the scramble version of gp91-dstat for 20 min before and during ES. In *wt* myotubes, gp91-dstat treatment blocked depolarization-induced IL-6 mRNA increases (Fig. 5C) while the scramble version of gp91-dstat had no effect. In *mdx* myotubes gp91-dstat treatment prevented the previously observed decreases in IL-6 mRNA induced by ES (Fig. 5C) and the scrambled version of gp91-dstat caused no significant change in IL-6 mRNA compared to control.

3.11. BAPTA-AM reduces IL-6 expression after ES in wt without any effect in mdx myotubes

To study the relationship between intracellular Ca^{2+} and IL-6 gene expression induced by ES, we pre-incubated the myotubes with BAPTA-AM (30 μM) 30 min after ES. In *wt* myotubes BAPTA-AM reduced depolarization-induced IL-6 mRNA increases (Fig. 5D). In dystrophic muscle cells BAPTA-AM had no effect in IL-6 mRNA levels either at rest or in electrically stimulated conditions.

3.12. LPS increases NF-κB activity and IL-6 mRNA levels

Dystrophic mice have been shown to have high levels of serum IL-6 and increased skeletal muscle expression of IL-6 [10,11]. To evaluate the role of the inflammatory pathway as a mechanism for this increase we studied the effect of lipopolysaccharide (LPS, 1 μg/mL) on both NF-κB activity and IL-6 mRNA levels in dystrophic myotubes. LPS dramatically increased NF-κB transcriptional activity assessed by a luciferase reporter, at 12 h in both *wt* and *mdx* myotubes ($P < 0.001$), but the effect was larger in *mdx* myotubes than in *wt* (Fig. S2). Furthermore, IL-6 expression was substantially increased 2 h after stimulation in both *wt* and

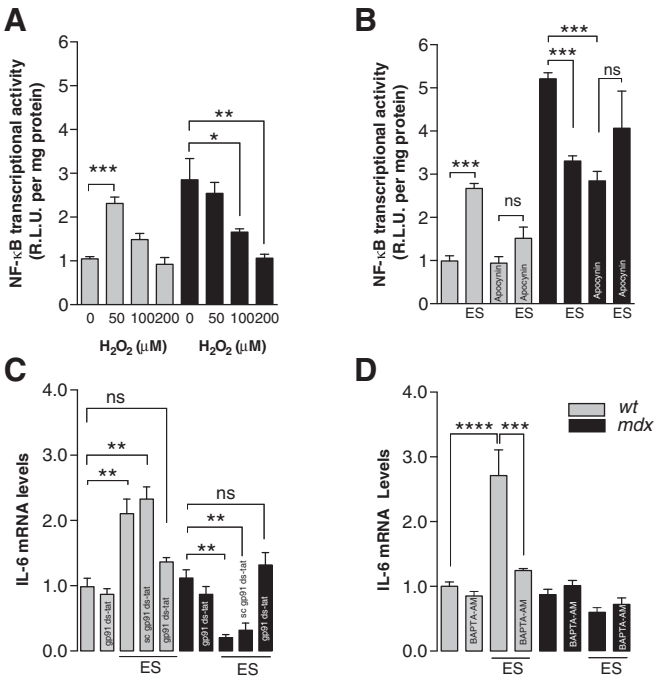

Fig. 5. NF-κB dysregulation after membrane depolarization in *mdx* myotubes is mediated by excessive ROS production. A. NF-κB activity induced by H_2O_2 in *wt* and *mdx* myotubes. Cells were stimulated with different concentrations of exogenous H_2O_2. Luciferase activity was determined after 12 h (n = 3). B. NOX2 inhibition (apocynin) blunted depolarization-induced changes in NF-κB activity in both *wt* and *mdx* myotubes (n = 3). C. NOX2 inhibition blocked depolarization-induced changes in IL-6 expression in both *wt* and *mdx* myotubes (n = 3). D. BAPTA-AM (30 μM) blocked depolarization-induced changes in IL-6 expression in both *wt* myotubes. * = $P < 0.05$, ** = $P < 0.01$, and *** = $P < 0.001$ (indicated or versus basal *wt* value), and ns, no significant difference.

mdx muscle cells ($P < 0.001$ and $P < 0.01$ respectively) (Fig. S1). These data suggest that despite the fact that NF-κB activation and IL-6 expression are impaired after ES in dystrophic myotubes, their ability to respond to the inflammatory pathway is intact.

4. Discussion

IL-6 is an important myokine released during exercise by the skeletal muscles, playing an important role in muscle metabolism and regeneration induced by exercise. DMD pathology is characterized by a persistent inflammatory response in the skeletal muscles due to chronic damage. There is a basal increment of IL-6 levels in plasma and muscle lysates from DMD patients; however the contribution of skeletal muscle fibers to this pool after exercise is unknown. The aim of this research was to study the molecular mechanism involved in IL-6 expression evoked by ES in dystrophic muscle cells. Our main results are that 1) depolarization-induced IL-6 expression is controlled by NOX2/NF-κB pathway in normal skeletal muscle. 2) Dystrophic skeletal muscle cells fail to increase IL-6 after depolarization and exercise. 3) Both altered ROS production and NF-κB activity appear to be involved in the lack of IL-6 response to exercise in *mdx* myotubes.

NADPH oxidase complex is expressed in normal skeletal muscle and represents the main ROS source during resting and contracting conditions [18–20]. Here, we showed that ROS production after electrical stimuli was higher in *mdx* muscle cells and can be effectively blocked by NOX2 inhibitors (Fig. 3C). The fact that the effect of NOX2 inhibitors appears to be higher in *mdx* cells suggests that the proportion of ROS produced by NOX2 is also higher in these cells. Our results are in agreement with previous findings that ROS production induced by muscle stretching is higher in *mdx* fibers compared to *wt* fibers [23,35]. These data suggest that increments of ROS during muscle activity may contribute to oxidative stress and signaling dysregulation observed in DMD pathology [36]. Moreover, gene expression of key subunits for NADPH oxidase activity, $p47^{phox}$ and $gp91^{phox}$ were upregulated in *mdx* myotubes (Fig. 4D and E). These data were supported by a 9-fold increase in protein expression for the catalytic subunit $gp91^{phox}$ in *mdx* myotubes at resting conditions (Fig. 4F and G). Previous studies showed an increased expression of NADPH oxidase subunits in dystrophic *mdx flexor digitorum brevis* [23], *tibialis anterior* [37] and diaphragm [38], where a participation of the immune system has been suggested [23]. In this study, we showed in an immune cell-free system that dystrophin deficiency leads to an increased NADPH oxidase expression.

NF-κB family plays an essential role in normal response to cellular stress in the skeletal muscle including *redox* signaling [39]. We previously showed that basal NF-κB activity is increased in *mdx* muscle cells as a result of an elevated resting Ca^{2+} concentration [12]. Here, we confirmed these findings and we demonstrated that NF-κB signaling is upregulated under resting conditions in *mdx* myotubes through IκBα degradation (Fig. 1D). The increased resting intracellular calcium concentration observed in dystrophic myotubes [12,38] may involve calpain activation and the subsequent IκBα degradation [40]. On the other hand, a decreased basal p65 phosphorylation at Ser536 was observed in *mdx* myotubes (Fig. 1B), these results suggest that basal NF-κB activity in *mdx* myotubes in the absence of immune mediators [41] does not require phosphorylation at Ser536.

In human skeletal muscles, NF-κB has been shown to be activated after resistance exercise [42], cycling [43], eccentric muscle contraction [44], or ES [16,45]. In this work, we showed that membrane depolarization increased NF-κB activity in normal cells (Fig. 1B), as we previously reported in rat myotubes [16], but this physiological response is not observed in dystrophic muscle cells. In *wt* myotubes an increase in p-p65 was observed after membrane depolarization that was correlated with an increase in NF-κB transcriptional activity measured by NF-κB driven luciferase reporters (Fig. 1E).

Our laboratory has reported that depolarization-induced NF-κB activation is partially blocked by the antioxidant *N*-acetyl cysteine (NAC) [16]. In the present study, apocynin treatment prevented depolarization-induced NF-κB activation in *wt* myotubes (Fig. 5B), showing the importance of ROS production suggested in previous studies [23]. In contrast, in *mdx* cells the reduction of NF-κB activation after ES was blocked by apocynin treatment, showing that physiological NOX2-dependent ROS production is necessary to positively modulate NF-κB signaling (Fig. 5B). We hypothesize that the elevated ROS levels at resting conditions and the increase produced by membrane depolarization impair the NF-κB function in dystrophic cells. This hypothesis is supported by the fact that lower doses of H_2O_2 increased NF-κB activity whereas higher doses have no effect in *wt* myotubes but that in dystrophic muscle cells, low doses had no effect but higher concentrations of H_2O_2 reduced NF-κB transcriptional activity (Fig. 5A). ROS can both activate or repress NF-κB signaling depending on the cell type, levels and localization (reviewed in [34]). ROS stimulate NF-κB pathway in the cytosol, whereas inhibit its activity in the nucleus. Elevated ROS may inhibit NF-κB binding ability due to a cysteine oxidation in the p50 subunit. Moreover, oxidation of IKK on Cys-179 inactivates NF-κB signaling. There are many examples in the literature for NF-κB inhibition by ROS [34]. Considering the elevated levels of NO due to iNOS [12] in *mdx* muscles and the increase of ROS after membrane depolarization it is possible that these redox modifications may impair the NF-κB signaling pathway [48,49].

After depolarization with our stimulation protocol (one train, 250 pulses at 20 Hz), we found that IκBα levels remain similar to untreated cells (Fig. 1A). There is some evidence showing that p65 phosphorylation at Ser536 targets to an IκBα independent pathway for NF-κB activation [46]. A reduced binding of NF-κB to IκB due to increased

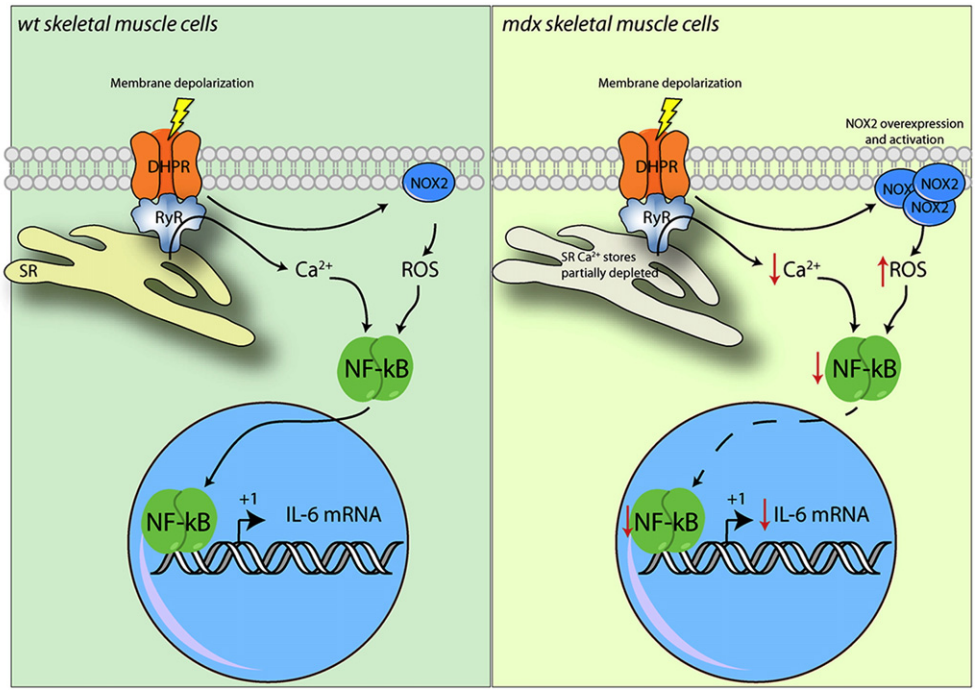

Fig. 6. Proposed model for NF-κB and IL-6 dysregulation in dystrophic myotubes. In *wt* skeletal muscle cells (left panel) membrane depolarization increase NOX2-dependent ROS production and triggers Ca^{2+} release from intracellular reservoirs. Both Ca^{2+} and ROS levels are necessary to increase NF-κB transcriptional activity, and subsequently IL-6 gene expression. In *mdx* skeletal muscle cells (right panel), NOX2 overexpression increase ROS levels after membrane depolarization that negatively affects NF-κB transcriptional activity and IL-6 mRNA levels. In addition, Ca^{2+} signals elicited by membrane depolarization that are necessary for NF-κB activation are significantly reduced. IL-6 is a key regulator of metabolism and participates in the coordination of several organs during exercise. The impairment in IL-6 production might exacerbate muscle dysfunction in patients with DMD.

phosphorylation at ser536 of p65 subunit of NF-κB has been reported in response to H_2O_2 [50,51]. Moreover, it has been reported that NF-κB activation without IκBα degradation, due to IκBα association to PI3K leading NF-κB to migrate to the nucleus [47]. Moreover, our lab previously demonstrated that IκBα degradation depends on the frequency and duration of the stimuli [16].

ROS have been linked with IL-6 expression [15] and there is evidence showing that antioxidant administration might reduce IL-6 release by the skeletal muscle [52]. However, the source of ROS involved in this process is unclear. Our results showed that in *wt* cells, inhibition of NOX2 by the mimetic peptide gp91-dstat reduces IL-6 expression. In contrast, in *mdx* cell inhibition of NOX2 prevents repression of IL-6 expression after ES. Collectively, our data suggest that an excessive NOX2-mediated ROS production inhibits the NF-κB-dependent transcription of IL-6 gene, ablating its expression after membrane depolarization and impairing its secretion.

Our results demonstrate that IL-6 secretion is elevated in resting conditions in *mdx* myotubes, but mRNA levels are similar to those observed in *wt* myotubes. This can be achieved at different levels of regulation (e.g. post-transcriptional, translational, or secretion route). These basal differences might be due to an altered secretion of preformed IL-6 pool; although this was not the aim of this work, this is an interesting finding because it may reflect and altered IL-6 secretion similar to the one observed in plasma and muscle lysates in DMD [3,4]. Our data suggest that dystrophic skeletal muscle cells fail to express and secrete IL-6 in response to membrane depolarization or exercise. IL-6 is an endocrine, paracrine, and autocrine-signaling molecule. It is essential for a normal response to exercise, acting as an important metabolic regulator [13,29]. Thus, its alteration in dystrophic muscle cells can affect the normal response to contractile activity and impair muscle function [53,54]. Moreover, studies in rodents have shown that IL-6 contributes to muscle regeneration or hypertrophy after injury which may involve a similar stimulatory effect on satellite cell proliferation [55] and up-regulation of utrophin [56]. It seems that IL-6 has a dual effect in muscle physiology depending on its temporal release and concentration [31]. After membrane damage, muscle elevation of IL-6 appears to be due to leukocyte activation (mast cells, neutrophils, monocytes and macrophages) and it is necessary for muscle repair [57]. IL-6 null mice showed an abnormal muscle repair, pointing to the importance of this cytokine in the regeneration process [58]. Moreover, blockade of IL-6 in *mdx* mice is deleterious supporting this hypothesis [59]. On the other hand, during exercise IL-6 is a key energetic regulator that coordinates multiple organs to fulfill the energetic muscle requirements [13]. IL-6 release is transient, peaking at the end of exercise and then returning to basal levels [31]. The absence of an IL-6 increase after exercise due to altered NF-κB signaling in dystrophic muscles could induce metabolic dysfunctions and lack of adaptation in the skeletal muscles that undergo physical activity. Contrary to ES response, stimulation with LPS induces activation of NF-κB and IL-6 expression in both skeletal myotubes (Fig. S1). These data suggest that despite the fact that NF-κB activation and IL-6 expression are impaired after ES in dystrophic myotubes, they are able to respond to the inflammatory stimuli.

The NF-κB molecular mechanisms that explain the differences in the response to LPS should be explored in future studies.

In summary, we have found that the IL-6 gene expression triggered by membrane depolarization is impaired in *mdx* myotubes, due to an increased NOX2-dependent ROS production and reduced NF-κB activation after depolarization (Fig. 6). This altered pathway may well be on the basis of reduced muscle regeneration and increased cell death associated with the absence of dystrophin, and may be generalizable to other muscle diseases as well.

Supplementary data to this article can be found online at http://dx.doi.org/10.1016/j.bbadis.2015.03.012.

Transparency document

The Transparency document associated with this article can be found, in the online version.

Acknowledgements

This work was supported by FONDECYT 1110467 (EJ) and ACT1111 (EJ) and FONDECYT 3140491 (DV). Research reported in this publication was supported in part by the National Institute of Arthritis and Musculoskeletal and Skin Diseases of the National Institutes of Health under Award Number AR43140 and AR052534 (JRL and PDA). The content is solely the responsibility of the authors and does not necessarily represent the official views of the National Institutes of Health.

References

[1] D.J. Blake, A. Weir, S.E. Newey, K.E. Davies, Function and genetics of dystrophin and dystrophin-related proteins in muscle, Physiol. Rev. 82 (2002) 291–329.
[2] A.E. Emery, The muscular dystrophies, Lancet 359 (2002) 687–695.
[3] R. Sockolov, B. Irwin, R.H. Dressendorfer, E.M. Bernauer, Exercise performance in 6- to-11-year-old boys with Duchenne muscular dystrophy, Arch. Phys. Med. Rehabil. 58 (1977) 195–201.
[4] M. Sandri, M. Podhorska-Okolow, V. Geromel, C. Rizzi, P. Arslan, C. Franceschi, U. Carraro, Exercise induces myonuclear ubiquitination and apoptosis in dystrophin-deficient muscle of mice, J. Neuropathol. Exp. Neurol. 56 (1997) 45–57.
[5] J.T. Vilquin, V. Brussee, I. Asselin, I. Kinoshita, M. Gingras, J.P. Tremblay, Evidence of mdx mouse skeletal muscle fragility in vivo by eccentric running exercise, Muscle Nerve 21 (1998) 567–576.
[6] B.S. Gordon, D.A. Lowe, M.C. Kostek, Exercise increases utrophin protein expression in the mdx mouse model of Duchenne muscular dystrophy, Muscle Nerve 49 (2014) 915–918.
[7] N.P. Evans, S.A. Misyak, J.L. Robertson, J. Bassaganya-Riera, R.W. Grange, Immune-mediated mechanisms potentially regulate the disease time-course of Duchenne muscular dystrophy and provide targets for therapeutic intervention, PM R 1 (2009) 755–768.
[8] J.G. Tidball, Inflammatory processes in muscle injury and repair, Am. J. Physiol. Regul. Integr. Comp. Physiol. 288 (2005) R345–R353.
[9] J. Scheller, A. Chalaris, D. Schmidt-Arras, S. Rose-John, The pro- and anti-inflammatory properties of the cytokine interleukin-6, Biochim. Biophys. Acta 1813 (2011) 878–888.
[10] J.B. Kurek, S. Nouri, G. Kannourakis, M. Murphy, L. Austin, Leukemia inhibitory factor and interleukin-6 are produced by diseased and regenerating skeletal muscle, Muscle Nerve 19 (1996) 1291–1301.
[11] S. Messina, G.L. Vita, M. Aguennouz, M. Sframeli, S. Romeo, C. Rodolico, G. Vita, Activation of NF-kappaB pathway in Duchenne muscular dystrophy: relation to age, Acta Myol. 30 (2011) 16–23.
[12] F. Altamirano, J.R. Lopez, C. Henriquez, T. Molinski, P.D. Allen, E. Jaimovich, Increased resting intracellular calcium modulates NF-kappaB-dependent inducible nitric-oxide synthase gene expression in dystrophic mdx skeletal myotubes, J. Biol. Chem. 287 (2012) 20876–20887.
[13] B.K. Pedersen, Muscular interleukin-6 and its role as an energy sensor, Med. Sci. Sports Exerc. 44 (2012) 392–396.
[14] N. Juretic, P. Garcia-Huidobro, J.A. Iturrieta, E. Jaimovich, N. Riveros, Depolarization-induced slow Ca^{2+} transients stimulate transcription of IL-6 gene in skeletal muscle cells, Am. J. Physiol. Cell Physiol. 290 (2006) C1428–C1436.
[15] I. Kosmidou, T. Vassilakopoulos, A. Xagorari, S. Zakynthinos, A. Papapetropoulos, C. Roussos, Production of interleukin-6 by skeletal myotubes: role of reactive oxygen species, Am. J. Respir. Cell Mol. Biol. 26 (2002) 587–593.
[16] J.A. Valdes, J. Hidalgo, J.L. Galaz, N. Puentes, M. Silva, E. Jaimovich, M.A. Carrasco, NF-kappaB activation by depolarization of skeletal muscle cells depends on ryanodine and IP3 receptor-mediated calcium signals, Am. J. Physiol. Cell Physiol. 292 (2007) C1960–C1970.
[17] M.C. Gomez-Cabrera, E. Domenech, J. Vina, Moderate exercise is an antioxidant: up-regulation of antioxidant genes by training, Free Radic. Biol. Med. 44 (2008) 126–131.
[18] G.K. Sakellariou, A. Vasilaki, J. Palomero, A. Kayani, L. Zibrik, A. McArdle, M.J. Jackson, Studies of mitochondrial and nonmitochondrial sources implicate nicotinamide adenine dinucleotide phosphate oxidase(s) in the increased skeletal muscle superoxide generation that occurs during contractile activity, Antioxid. Redox Signal. 18 (2013) 603–621.
[19] L.P. Michaelson, G. Shi, C.W. Ward, G.G. Rodney, Mitochondrial redox potential during contraction in single intact muscle fibers, Muscle Nerve 42 (2010) 522–529.
[20] R. Pal, P. Basu Thakur, S. Li, C. Minard, G.G. Rodney, Real-time imaging of NADPH oxidase activity in living cells using a novel fluorescent protein reporter, PLoS One 8 (2013) e63989.
[21] C. Hidalgo, G. Sanchez, G. Barrientos, P. Aracena-Parks, A transverse tubule NADPH oxidase activity stimulates calcium release from isolated triads via ryanodine receptor type 1 S-glutathionylation, J. Biol. Chem. 281 (2006) 26473–26482.
[22] R. Pal, M. Palmieri, J.A. Loehr, S. Li, R. Abo-Zahrah, T.O. Monroe, P.B. Thakur, M. Sardiello, G.G. Rodney, Src-dependent impairment of autophagy by oxidative stress in a mouse model of Duchenne muscular dystrophy, Nat. Commun. 5 (2014) 4425.
[23] N.P. White, E.W. Yeung, S.C. Froehner, D.G. Allen, Skeletal muscle NADPH oxidase is increased and triggers stretch-induced damage in the mdx mouse, PLoS One 5 (2010) e15354.
[24] T.A. Rando, H.M. Blau, Primary mouse myoblast purification, characterization, and transplantation for cell-mediated gene therapy, J. Cell Biol. 125 (1994) 1275–1287.
[25] M. Casas, F. Altamirano, E. Jaimovich, Myogenesis: Methods and Protocols, 1st ed. Humana Press, 2011.
[26] G. Jorquera, F. Altamirano, A. Contreras-Ferrat, G. Almarza, S. Buvinic, V. Jacquemond, E. Jaimovich, M. Casas, Cav1.1 controls frequency-dependent events regulating adult skeletal muscle plasticity, J. Cell Sci. 126 (2013) 1189–1198.
[27] K.J. Livak, T.D. Schmittgen, Analysis of relative gene expression data using real-time quantitative PCR and the 2(−delta delta C(T)) method, Methods 25 (2001) 402–408.
[28] O.J. Marshall, PerlPrimer: cross-platform, graphical primer design for standard, bisulphite and real-time PCR, Bioinformatics 20 (2004) 2471–2472.
[29] S.S. Welc, T.L. Clanton, The regulation of interleukin-6 implicates skeletal muscle as an integrative stress sensor and endocrine organ, Exp. Physiol. 98 (2013) 359–371.
[30] Y.Z. Lin, S.Y. Yao, R.A. Veach, T.R. Torgerson, J. Hawiger, Inhibition of nuclear translocation of transcription factor NF-kappa B by a synthetic peptide containing a cell membrane-permeable motif and nuclear localization sequence, J. Biol. Chem. 270 (1995) 14255–14258.
[31] B.K. Pedersen, Muscle as a secretory organ, Compr. Physiol. 3 (2013) 1337–1362.
[32] D. Riquelme, A. Alvarez, N. Leal, T. Adasme, I. Espinoza, J.A. Valdes, N. Troncoso, S. Hartel, J. Hidalgo, C. Hidalgo, M.A. Carrasco, High-frequency field stimulation of primary neurons enhances ryanodine receptor-mediated Ca^{2+} release and generates hydrogen peroxide, which jointly stimulate NF-kappaB activity, Antioxid. Redox Signal. 14 (2011) 1245–1259.
[33] G.K. Sakellariou, M.J. Jackson, A. Vasilaki, Redefining the major contributors to superoxide production in contracting skeletal muscle. The role of NAD(P)H oxidases, Free Radic. Res. 48 (2014) 12–29.
[34] M.J. Morgan, Z.G. Liu, Crosstalk of reactive oxygen species and NF-kappaB signaling, Cell Res. 21 (2011) 103–115.
[35] R.J. Khairallah, G. Shi, F. Sbrana, B.L. Prosser, C. Borroto, M.J. Mazaitis, E.P. Hoffman, A. Mahurkar, F. Sachs, Y. Sun, Y.W. Chen, R. Raiteri, W.J. Lederer, S.G. Dorsey, C.W. Ward, Microtubules underlie dysfunction in Duchenne muscular dystrophy, Sci. Signal. 5 (2012) ra56.
[36] R.J. Ragusa, C.K. Chow, J.D. Porter, Oxidative stress as a potential pathogenic mechanism in an animal model of Duchenne muscular dystrophy, Neuromuscul. Disord. 7 (1997) 379–386.
[37] V.M. Shkryl, A.S. Martins, N.D. Ullrich, M.C. Nowycky, E. Niggli, N. Shirokova, Reciprocal amplification of ROS and Ca(2+) signals in stressed mdx dystrophic skeletal muscle fibers, Pflugers Arch. 458 (2009) 915–928.
[38] F. Altamirano, D. Valladares, C. Henriquez-Olguin, M. Casas, J.R. Lopez, P.D. Allen, E. Jaimovich, Nifedipine treatment reduces resting calcium concentration, oxidative and apoptotic gene expression, and improves muscle function in dystrophic mdx mice, PLoS One 8 (2013) e81222.
[39] F. Mourkioti, N. Rosenthal, NF-kappaB signaling in skeletal muscle: prospects for intervention in muscle diseases, J. Mol. Med. 86 (2008) 747–759.
[40] K. Schaecher, J.M. Goust, N.L. Banik, The effects of calpain inhibition on IkB alpha degradation after activation of PBMCs: identification of the calpain cleavage sites, Neurochem. Res. 29 (2004) 1443–1451.
[41] S. Acharyya, S.A. Villalta, N. Bakkar, T. Bupha-Intr, P.M. Janssen, M. Carathers, Z.W. Li, A.A. Beg, S. Ghosh, Z. Sahenk, M. Weinstein, K.L. Gardner, J.A. Rafael-Fortney, M. Karin, J.G. Tidball, A.S. Baldwin, D.C. Guttridge, Interplay of IKK/NF-kappaB signaling in macrophages and myofibers promotes muscle degeneration in Duchenne muscular dystrophy, J. Clin. Invest. 117 (2007) 889–901.
[42] L. Vella, M.K. Caldow, A.E. Larsen, D. Tassoni, P.A. Della Gatta, P. Gran, A.P. Russell, D. Cameron-Smith, Resistance exercise increases NF-kappaB activity in human skeletal muscle, Am. J. Physiol. Regul. Integr. Comp. Physiol. 302 (2012) R667–R673.
[43] P. Tantiwong, K. Shanmugasundaram, A. Monroy, S. Ghosh, M. Li, R.A. DeFronzo, E. Cersosimo, A. Sriwijitkamol, S. Mohan, N. Musi, NF-kappaB activity in muscle from obese and type 2 diabetic subjects under basal and exercise-stimulated conditions, Am. J. Physiol. Endocrinol. Metab. 299 (2010) E794–E801.
[44] R.D. Hyldahl, L. Xin, M.J. Hubal, S. Moeckel-Cole, S. Chipkin, P.M. Clarkson, Activation of nuclear factor-kappaB following muscle eccentric contractions in humans is localized primarily to skeletal muscle-residing pericytes, FASEB J. 25 (2011) 2956–2966.
[45] M. Scheler, M. Irmler, S. Lehr, S. Hartwig, H. Staiger, H. Al-Hasani, J. Beckers, M. Hrabe de Angelis, H.U. Haring, C. Weigert, The cytokine response of primary human myotubes in an in vitro exercise model, Am. J. Physiol. Cell Physiol. 305 (8) (2013) C877–C886.
[46] C.Y. Sasaki, T.J. Barberi, P. Ghosh, D.L. Longo, Phosphorylation of RelA/p65 on serine 536 defines an I{kappa}B{alpha}-independent NF-{kappa}B pathway, J. Biol. Chem. 280 (2005) 34538–34547.
[47] C. Beraud, W.J. Henzel, P.A. Baeuerle, Involvement of regulatory and catalytic subunits of phosphoinositide 3-kinase in NF-kappaB activation, Proc. Natl. Acad. Sci. U. S. A. 96 (1999) 429–434.
[48] Z.T. Kelleher, A. Matsumoto, J.S. Stamler, H.E. Marshall, NOS2 regulation of NF-kappaB by S-nitrosylation of p65, J. Biol. Chem. 282 (2007) 30667–30672.
[49] J.R. Matthews, C.H. Botting, M. Panico, H.R. Morris, R.T. Hay, Inhibition of NF-kappaB DNA binding by nitric oxide, Nucleic Acids Res. 24 (1996) 2236–2242.
[50] S. Nakajima, M. Kitamura, Bidirectional regulation of NF-kappaB by reactive oxygen species: a role of unfolded protein response, Free Radic. Biol. Med. 65 (2013) 162–174.
[51] E. Kefaloyianni, C. Gaitanaki, I. Beis, ERK1/2 and p38-MAPK signalling pathways, through MSK1, are involved in NF-kappaB transactivation during oxidative stress in skeletal myoblasts, Cell. Signal. 18 (2006) 2238–2251.
[52] C.P. Fischer, N.J. Hiscock, M. Penkowa, S. Basu, B. Vessby, A. Kallner, L.B. Sjoberg, B.K. Pedersen, Supplementation with vitamins C and E inhibits the release of interleukin-6 from contracting human skeletal muscle, J. Physiol. 558 (2004) 633–645.

[53] J.A. Call, J.N. McKeehen, S.A. Novotny, D.A. Lowe, Progressive resistance voluntary wheel running in the mdx mouse, Muscle Nerve 42 (2010) 871–880.
[54] R.M. Landisch, A.M. Kosir, S.A. Nelson, K.A. Baltgalvis, D.A. Lowe, Adaptive and non-adaptive responses to voluntary wheel running by mdx mice, Muscle Nerve 38 (2008) 1290–1303.
[55] A.L. Serrano, B. Baeza-Raja, E. Perdiguero, M. Jardi, P. Munoz-Canoves, Interleukin-6 is an essential regulator of satellite cell-mediated skeletal muscle hypertrophy, Cell Metab. 7 (2008) 33–44.
[56] K. Fujimori, Y. Itoh, K. Yamamoto, Y. Miyagoe-Suzuki, K. Yuasa, K. Yoshizaki, H. Yamamoto, S. Takeda, Interleukin 6 induces overexpression of the sarcolemmal utrophin in neonatal mdx skeletal muscle, Hum. Gene Ther. 13 (2002) 509–518.
[57] N.J. Pillon, P.J. Bilan, L.N. Fink, A. Klip, Cross-talk between skeletal muscle and immune cells: muscle-derived mediators and metabolic implications, Am. J. Physiol. Endocrinol. Metab. 304 (2013) E453–E465.
[58] C. Zhang, Y. Li, Y. Wu, L. Wang, X. Wang, J. Du, Interleukin-6/signal transducer and activator of transcription 3 (STAT3) pathway is essential for macrophage infiltration and myoblast proliferation during muscle regeneration, J. Biol. Chem. 288 (2013) 1489–1499.
[59] M.C. Kostek, K. Nagaraju, E. Pistilli, A. Sali, S.H. Lai, B. Gordon, Y.W. Chen, IL-6 signaling blockade increases inflammation but does not affect muscle function in the mdx mouse, BMC Musculoskelet. Disord. 13 (2012) 106.